

## Growth of single-crystalline, atomically smooth MgO films on Ge(001) by molecular beam epitaxy

Wei Han<sup>a,1</sup>, Yi Zhou<sup>b,1</sup>, Yong Wang<sup>c</sup>, Yan Li<sup>a</sup>, Jared.J.I. Wong<sup>a</sup>, K. Pi<sup>a</sup>, A.G. Swartz<sup>a</sup>, K.M. McCreary<sup>a</sup>, Faxian Xiu<sup>b</sup>, Kang L. Wang<sup>b</sup>, Jin Zou<sup>c</sup>, R.K. Kawakami<sup>a,\*</sup>

<sup>a</sup> Department of Physics and Astronomy, University of California, Riverside, CA 92521, USA

<sup>b</sup> Device Research Laboratory, Department of Electrical Engineering, University of California, Los Angeles, CA 90095, USA

<sup>c</sup> School of Engineering and Center of Microscopy and Microanalysis, The University of Queensland, Brisbane, QLD 4072, Australia

### ARTICLE INFO

#### Article history:

Received 12 September 2009

Accepted 30 September 2009

Communicated by K.H. Ploog

Available online 7 October 2009

#### PACS:

68.55.aj

81.15.Hi

61.05.jh

85.75.-d

#### Keywords:

A3. Molecular beam epitaxy

B1. Ge

B1. MgO

B3. Spintronics

### ABSTRACT

We investigate the growth of MgO thin films on Ge(001) via molecular beam epitaxy and find that the growth temperature plays a key role in the quality of MgO thin films. Reflection high-energy electron diffraction (RHEED) and atomic force microscopy show that the single-crystal quality and atomically smooth morphology are optimized for a growth temperature of 250 °C. RHEED and transmission electron microscopy indicate that the MgO is (001) oriented and the MgO unit cell has a 45° in-plane rotation with respect to that of Ge, providing a high-quality film and interface for potential spin-injection experiments.

© 2009 Elsevier B.V. All rights reserved.

## 1. Introduction

Semiconductor spintronics aims to add novel functionality to electronic devices by utilizing the spin degree of freedom [1]. Group-IV semiconductors are of particular interest due to the potential compatibility with established silicon technologies, and Ge has shown favorable properties related to magnetic doping [2–7]. One of the main challenges for Ge-based spintronics is to achieve efficient spin injection from ferromagnetic (FM) metal contacts into Ge. A promising avenue is to develop single-crystalline FM/MgO/Ge(001) heterostructures. In addition to alleviating the conductivity mismatch problem by introducing a tunnel barrier [8–10], MgO(001) films possess a special spin-filtering property based on wavefunction symmetry that greatly enhances the spin polarization when the FM is bcc Co<sub>x</sub>Fe<sub>1-x</sub> (up to 85% spin polarization in some cases) [11–14]. When applied to spin injection into GaAs, the FM/MgO/GaAs(001) system has exhibited very high spin-injection efficiency in spin-LED experi-

ments [15,16]; hence, the MgO barrier is potentially beneficial for spin injection into Ge. Furthermore, the MgO can act as a barrier to prevent diffusion of transition metals into Ge. The insertion of a thin layer of insulator can also alleviate the strong Fermi-level pinning problem of metal/n-Ge contacts [17–19]. While the growth of MgO on Si(001) and GaAs(001) has been well studied [16,20–24], very little work has been done on Ge(001). Therefore, the epitaxial growth of MgO thin films on Ge(001) is an important issue for the development of Ge-based spintronics.

In this paper, we demonstrate the growth of atomically smooth, single-crystalline MgO thin films on Ge(001) by molecular beam epitaxy (MBE). Using *in situ* reflection high energy electron diffraction (RHEED) and atomic force microscopy (AFM) to characterize the crystal structure and morphology, we find that the growth temperature plays a key role in determining the quality of the MgO film. The sharpest RHEED patterns are obtained for a growth temperature of 250 °C and the root-mean-square (rms) roughness measured by AFM is 0.17 nm, which is less than the atomic spacing of MgO (0.2106 nm). Deposition at room temperature (RT) or 400 °C produces much rougher films. High resolution transmission electron microscopy (HRTEM) is used to characterize the single-crystal structure, atomic-scale morphology, and interfacial structure of Fe/MgO/Ge(001). Interestingly,

\* Corresponding author. Tel.: +1951 827 5343; fax: +1951 827 4529.

E-mail address: roland.kawakami@ucr.edu (R.K. Kawakami).

<sup>1</sup> These authors have contributed equally to this work.

the MgO is (001) oriented with a  $45^\circ$  in-plane rotation of the unit cell relative to that of Ge(001). This achieves the relatively small lattice mismatch of 5.5%, as opposed to a  $\sim 25\%$  mismatch that would result from a cube-on-cube alignment as often seen in MgO/Si(001) and MgO/GaAs(001) [16,20–24].

## 2. Experimental details

Samples are grown by MBE in an ultrahigh vacuum (UHV) system with a base pressure of  $1 \times 10^{-10}$  Torr. The wafers are first cleaned in isopropyl alcohol, followed by successive washes in dilute  $\text{NH}_4\text{OH}$ , dilute  $\text{H}_2\text{SO}_4$ , and  $\text{H}_2\text{O}_2$ . The  $\text{H}_2\text{O}_2$  produces a thin oxide protection layer on the Ge substrate. In the MBE chamber, the Ge substrate is annealed at  $500^\circ\text{C}$  for 1 h to remove the Ge-oxide layer prior to growth. Auger electron spectroscopy after the oxide desorption (Fig. 1, black curve) shows the peak for Ge (52 eV) but no oxygen peak at 505 eV, which confirms that the Ge-oxide layer is completely removed. The MgO is deposited by electron beam evaporation of a single-crystal MgO source. For potential spin-injection experiments, Fe and Al are deposited from thermal effusion cells. Typical deposition rates of  $\sim 1.5 \text{ \AA}/\text{min}$  for MgO,  $\sim 1.0 \text{ \AA}/\text{min}$  for Fe, and  $\sim 1.5 \text{ \AA}/\text{min}$  for Al are measured by a quartz deposition monitor.

## 3. Results and discussion

We first utilize RHEED to investigate the effect of growth temperature on the crystalline quality of MgO thin films on Ge(001). Fig. 2a shows the RHEED patterns of the Ge(001) substrate after oxide desorption for the in-plane [110] and [100] azimuths. The sharp and streaky RHEED patterns indicate a high-quality Ge surface. A series of 3 nm MgO/Ge(001) samples are grown at different substrate temperatures ranging from RT to  $400^\circ\text{C}$ . Figs. 2b–f show the RHEED patterns after the MgO deposition for growth temperatures of RT, 200, 250, 300, and  $400^\circ\text{C}$ , respectively. All RHEED patterns are taken after cooling the sample down to RT. With the exception of the  $400^\circ\text{C}$  growth, all RHEED patterns exhibit spots, which indicate single-crystalline ordering. Between RT and  $250^\circ\text{C}$ , the RHEED patterns become sharper and streakier with increase in growth temperature, indicating an improvement of the crystal structure and epitaxial growth of the MgO thin film. For the growth temperature of  $300^\circ\text{C}$ , the RHEED pattern starts to fade away and by  $400^\circ\text{C}$  the RHEED pattern vanishes. Thus, the crystal structure is optimized for a growth temperature of  $250^\circ\text{C}$ . The RHEED patterns also indicate that the MgO has (001) orientation with a  $45^\circ$  rotation of

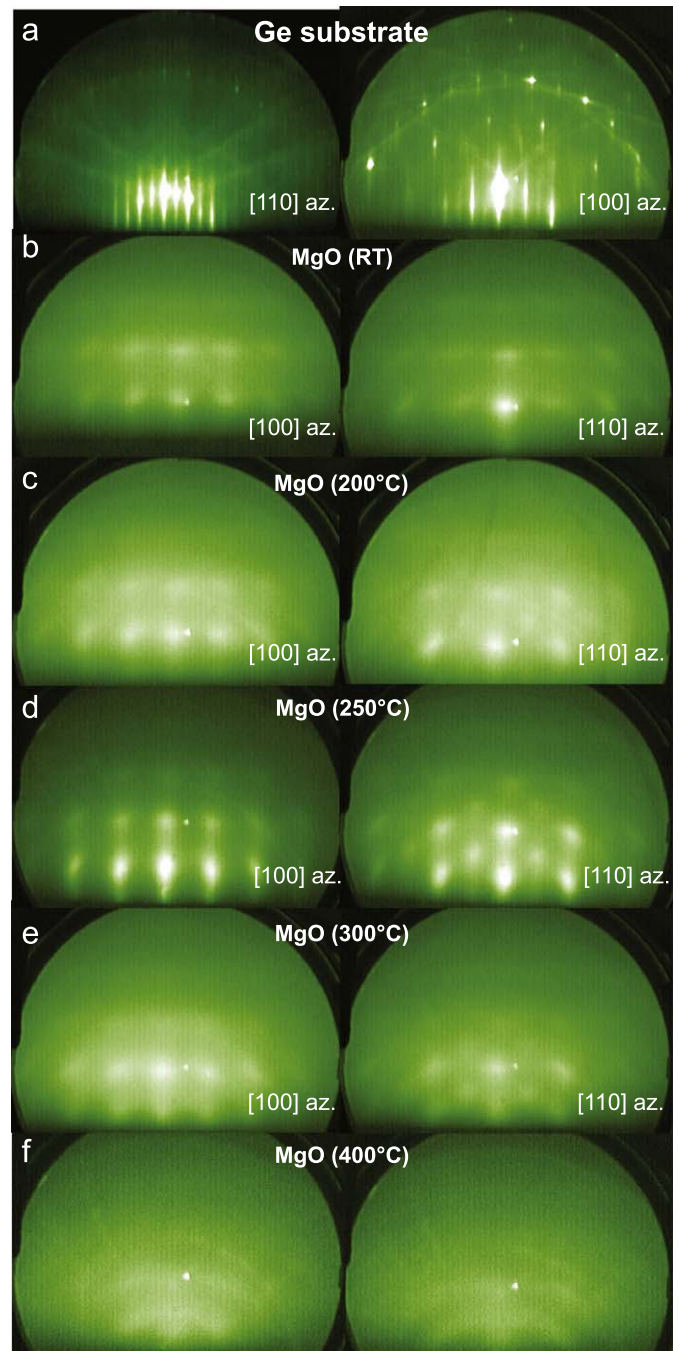


**Fig. 2.** RHEED patterns of Ge substrate and 3 nm MgO grown on Ge at different temperatures (left column in the Ge[110](001) and MgO[100](001) orientation; right column in the Ge[100](001) and MgO[110](001) orientation): (a) Ge substrate; (b) 3 nm MgO grown on Ge at RT; (c) 3 nm MgO grown on Ge at  $200^\circ\text{C}$ ; (d) 3 nm MgO grown on Ge at  $250^\circ\text{C}$ ; (e) 3 nm MgO grown on Ge at  $300^\circ\text{C}$ ; and (f) 3 nm MgO grown on Ge at  $400^\circ\text{C}$ .

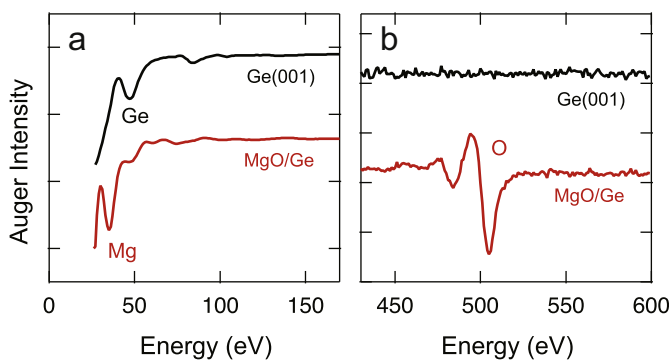


**Fig. 1.** Auger spectra of Ge substrate after annealing at  $500^\circ\text{C}$  for 1 h (black curve) and the typical spectra of 3 nm MgO grown on Ge substrate (red/grey curve): (a) the energy from 0 to 170 eV and (b) the energy from 430 to 600 eV.

the unit cell relative to the Ge(001) unit cell (i.e.  $\text{MgO}[100](001)\parallel\text{Ge}[110](001)$  as indicated in Fig. 2), which will be discussed in detail later.

Prior to removing the samples from UHV, Auger electron spectroscopy is performed on the MgO films. Fig. 1 (red/grey curve) shows a typical Auger spectrum of a 3 nm MgO film grown on Ge(001). Nearly identical spectra (with Mg peak at 35 eV and O peak at 505 eV) are observed for all growth temperatures. The key feature of the data is that the Mg peak appears at 35 eV (for

Mg in MgO crystal) as opposed to 45 eV (for elemental Mg), which demonstrates that MgO is being grown on the Ge substrate [25].

We utilize *ex situ* AFM to investigate the morphology of the MgO films grown at different temperatures. Fig. 3a shows the AFM image of the Ge substrate and Figs. 3b–e show the AFM images of 3 nm MgO grown on Ge(001) at RT, 250, 300, and 400 °C, respectively. Clearly, the growths at RT and 400 °C produce very rough MgO films, while the growths at 250 and 300 °C produce films with roughness comparable to the Ge substrate (rms roughness of 0.093 nm). Fig. 3f displays the rms roughness of the 3 nm MgO films as a function of growth temperature. Increase in the growth temperature from RT to 300 °C causes the rms roughness to decrease. Between 250 and 300 °C the MgO film is atomically smooth (rms roughness < 0.2106 nm, the atomic spacing of MgO). When the substrate temperature is above 300 °C, increase in the growth temperature results in a rougher MgO film. Based on the RHEED and AFM characterizations, the best single crystalline and atomically smooth MgO films are produced at a growth temperature of 250 °C.

Finally, we grow a complete Fe/MgO/Ge(001) heterostructure, which consists of Al(15 nm)/Fe(10 nm)/MgO(7 nm)/Ge(001), where the MgO is grown at 250 °C, the Fe is grown at 200 °C, and the Al is grown at RT. The Al-capping layer prevents oxidation of the Fe layer. Fig. 4a shows a cross-sectional HRTEM image, which confirms the single-crystal nature of the entire heterostructure. The atomic-scale morphology is smooth,

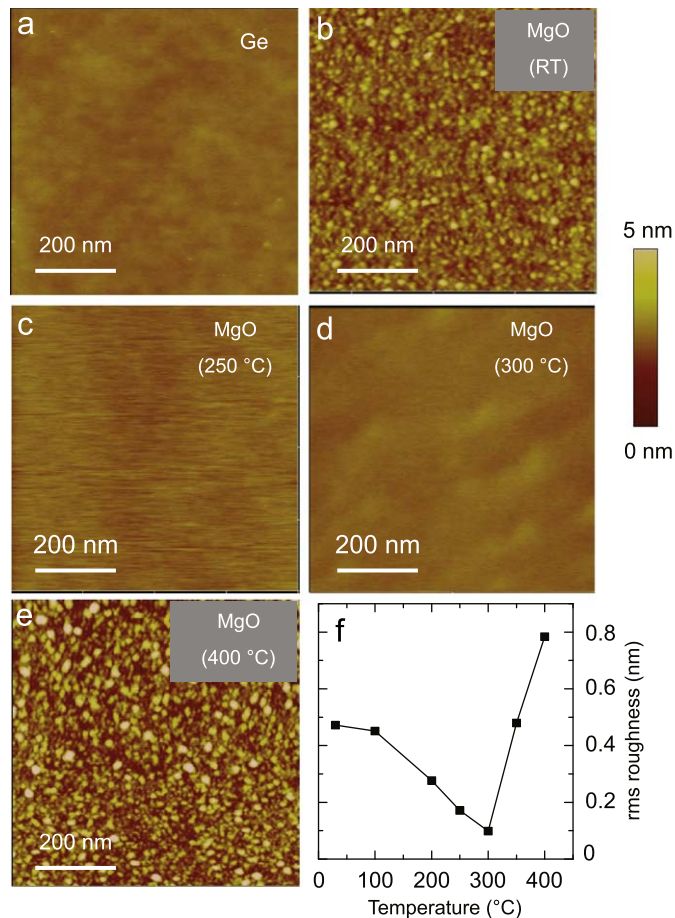


**Fig. 3.** AFM images of Ge substrate and 3 nm MgO grown on Ge at different temperatures: (a) initial Ge substrate; (b) 3 nm MgO grown on Ge at RT; (c) 3 nm MgO grown on Ge at 250 °C; (d) 3 nm MgO grown on Ge at 300 °C; (e) 3 nm MgO grown on Ge at 400 °C; and (f) rms roughness as a function of growth temperature.

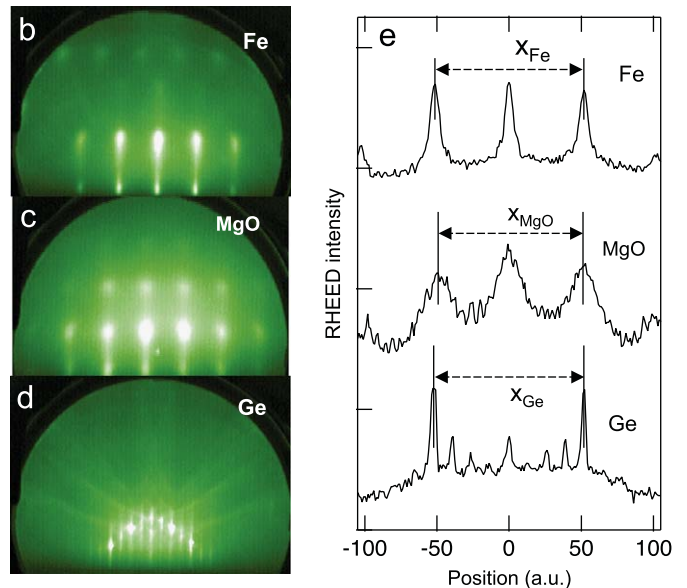
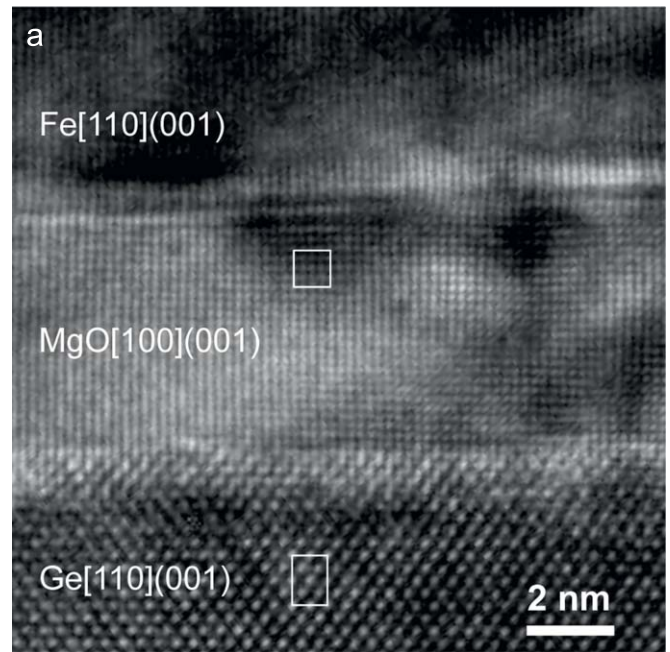


**Fig. 4.** HRTEM and RHEED of Fe/MgO/Ge(001): (a) HRTEM image of Fe/MgO/Ge; (b) RHEED pattern of 10 nm Fe; (c) RHEED pattern of 7 nm MgO; (d) RHEED pattern of Ge substrate; and (e) Line cuts of RHEED intensity of Fe, MgO, and Ge.  $x_{Fe}$ ,  $x_{MgO}$ ,  $x_{Ge}$  are the experimental RHEED peak-to-peak spacings.

consistent with the AFM studies (Fig. 3). The HRTEM reveals a transition region at the Ge and MgO interface of a few atomic layers. This is consistent with the MgO RHEED patterns, which begin to appear after ~0.5 nm of MgO deposition. The white squares drawn on the HRTEM image indicate that the projected unit cells are cubic for MgO and rectangular for Ge, which supports an epitaxial alignment of MgO[100]-(001) || Ge[110](001).

Figs. 4b–d show RHEED patterns measured for the Ge substrate (Fig. 4d), the MgO layer (Fig. 4c), and Fe layer (Fig. 4b) of the sample with the RHEED beam along the [110] azimuth of the Ge substrate. The sharp patterns are consistent with the single crystal, atomically smooth films as illustrated in the HRTEM images. Analysis of the RHEED patterns supports the epitaxial

relationship of Fe[110](001)||MgO[100](001)||Ge[110](001). The (001) orientation of the MgO and Fe layers is verified by the four-fold rotation symmetry of the RHEED patterns as the sample is rotated in-plane. The in-plane relationships are analyzed using line cuts of the RHEED patterns (Fig. 4e), where the spacing of the RHEED streaks is inversely proportional to the lateral spacing of the surface atoms. For the RHEED beam along [110] of Ge and the in-plane epitaxial relationship of Fe[110]||MgO[100]||Ge[110], the relevant surface lattice constants are  $a_{\text{Fe}}^* = 2a_{\text{Fe}}/\sqrt{2} = 0.4055$  nm,  $a_{\text{MgO}}^* = a_{\text{MgO}} = 0.4212$  nm,  $a_{\text{Ge}}^* = a_{\text{Ge}}/\sqrt{2} = 0.3992$  nm, where  $a_{\text{Fe}} = 0.2867$  nm,  $a_{\text{MgO}} = 0.4212$  nm, and  $a_{\text{Ge}} = 0.5646$  nm are the bulk lattice constants at room temperature. The bulk lattice constants lead to predicted RHEED spacing ratios of  $(a_{\text{Fe}}^*)^{-1}:(a_{\text{MgO}}^*)^{-1}:(a_{\text{Ge}}^*)^{-1} = 0.9845:0.9478:1$ . The experimental RHEED spacings from Fig. 4e have ratios of  $X_{\text{Fe}}:X_{\text{MgO}}:X_{\text{Ge}} = 0.9923:0.9644:1$ . The agreement between the predicted and measured RHEED spacings strongly supports the in-plane epitaxial relationship of Fe[110]||MgO[100]||Ge[110].

We note that the 45° in-plane rotation of MgO on Ge(001) is rather interesting, as MgO/Si(001) and MgO/GaAs(001) are usually reported to have a cube-on-cube epitaxial relationship [16,20–24]. For cube-on-cube, the ~25% lattice mismatch is accommodated by having four MgO unit cells match up with three Si or GaAs unit cells, leading to dangling bonds at the interface. A possible advantage of the 45° in-plane rotation of the MgO/Ge(001) is the reduction of dangling bonds, which should be favorable for electronic and spintronic properties.

#### 4. Conclusions

In summary, we find that the growth temperature is a key factor in the growth MgO films on Ge(001). Based on RHEED and AFM, the single-crystal quality and atomic-scale smoothness are optimized for a growth temperature of 250 °C. Cross-sectional HRTEM images of Fe/MgO/Ge(001) heterostructures directly show the single-crystal structure, atomically smooth morphology, and relatively sharp interfaces. The rotation of 45° in-plane between MgO and Ge gives rise to a better lattice match and thus provides a high-quality film and interface for potential spin-injection experiments.

#### Acknowledgments

WH, YL, JJIW, KP, AS, KMM, and RKK acknowledge the support of NSF (CAREER DMR-0450037). YZ, FX, and KLW acknowledge the support from Intel and the Western Institution of Nanoelectronics (WIN) through NRI. YW and JZ acknowledge the support of the Australian Research Council.

#### References

- [1] S.A. Wolf, D.D. Awschalom, R.A. Buhrman, J.M. Daughton, S. von Molnar, M.L. Roukes, A.Y. Chtchelkanova, D.M. Treger, *Science* 294 (2001) 1488.
- [2] I. Appelbaum, B. Huang, D.J. Monsma, *Nature* 447 (2007) 295.
- [3] B.T. Jonker, G. Kioseoglou, A.T. Hanbicki, C.H. Li, P.E. Thompson, *Nature Physics* 3 (2007) 542.
- [4] R. Jansen, *Nature Physics* 3 (2007) 521.
- [5] Y.D. Park, A.T. Hanbicki, S.C. Erwin, C.S. Hellberg, J.M. Sullivan, J.E. Mattson, T.F. Ambrose, A. Wilson, G. Spanos, B.T. Jonker, *Science* 295 (2002) 651.
- [6] S. Cho, S. Choi, S.C. Hong, Y. Kim, J.B. Ketterson, B.-J. Kim, Y.C. Kim, J.-H. Jung, *Phys. Rev. B* 66 (2002) 033303.
- [7] F. Tsui, L. He, L. Ma, A. Tkachuk, Y.S. Chu, K. Nakajima, T. Chikyow, *Phys. Rev. Lett.* 91 (2003) 177203.
- [8] G. Schmidt, D. Ferrand, L.W. Molenkamp, A.T. Filip, B.J. van Wees, *Phys. Rev. B* 62 (2000) R4790.
- [9] E.I. Rashba, *Phys. Rev. B* 62 (2000) R16267.
- [10] A. Fert, H. Jaffres, *Phys. Rev. B* 64 (2001) 184420.
- [11] W.H. Butler, X.-G. Zhang, T.C. Schulthess, J.M. MacLaren, *Phys. Rev. B* 63 (2001) 054416.
- [12] Ph. Mavropoulos, N. Papanikolaou, P.H. Dederichs, *Phys. Rev. Lett.* 85 (2000) 1088.
- [13] S. Yuasa, T. Nagahama, A. Fukushima, Y. Suzuki, K. Ando, *Nature Materials* 3 (2004) 868.
- [14] S.S.P. Parkin, C. Kaiser, A. Panchula, P.M. Rice, B. Hughes, M. Samant, S.-H. Yang, *Nature Materials* 3 (2004) 862.
- [15] X. Jiang, R. Wang, R.M. Shelby, R.M. Macfarlane, S.R. Bank, J.S. Harris, S.S.P. Parkin, *Phys. Rev. Lett.* 94 (2005) 056601.
- [16] Y. Lu, V.G. Truong, P. Renucci, M. Tran, H. Jaffres, C. Deranlot, J.-M. George, A. Lemaitre, Y. Zheng, D. Demaille, P.-H. Binh, T. Amand, X. Marie, *Appl. Phys. Lett.* 93 (2008) 152102.
- [17] Y. Zhou, M. Ogawa, X. Han, K.L. Wang, *Appl. Phys. Lett.* 93 (2008) 202105.
- [18] T. Nishimura, K. Kita, A. Toriumi, *Appl. Phys. Express* 1 (2008) 051406.
- [19] M. Kobayashi, A. Kinoshita, K. Sarawat, H.-S.P. Wong, Y. Nishi, *Symp. VLSI Tech.* 54 (2008).
- [20] S. Kaneko, H. Funakubo, T. Kadowaki, Y. Hirabayashi, K. Akiyama, *Europhys. Lett.* 81 (2008) 46001.
- [21] G.X. Miao, J.Y. Chang, M.J. van Veenhuizen, K. Thiel, M. Seibt, G. Eilers, M. Munzenberg, J.S. Moodera, *Appl. Phys. Lett.* 93 (2008) 142511.
- [22] X.Y. Chen, K.H. Wong, C.L. Mak, X.B. Yin, M. Wang, J.M. Liu, Z.G. Liu, *J. Appl. Phys.* 91 (2002) 5728.
- [23] L.D. Chang, M.Z. Tseng, E.L. Hu, D.K. Fork, *Appl. Phys. Lett.* 60 (1992) 1753.
- [24] L.S. Hung, L.R. Zheng, T.N. Blanton, *Appl. Phys. Lett.* 60 (1992) 3129.
- [25] M. Suleman, E.B. Pattinson, *Surf. Sci.* 35 (1973) 75.